RC22829 (W0306-150) June 26, 2003
Materials Science

IBM Research Report

Transport and Exchange of Hydrogen Isotopes in Silicon Device-related Stacks

Cristiano Krug, Evgeni Gousev, Eduard Cartier, Theodore H. Zabel

IBM Research Division
Thomas J. Watson Research Center
P.O. Box 218
Yorktown Heights, NY 10598

Research Division
Almaden - Austin - Beijing - Delhi - Haifa - India - T. J. Watson - Tokyo - Zurich

Transport and exchange of hydrogen isotopes in silicon device-related stacks

C. Krug,* E. P. Gusev, E. A. Cartier, and T. H. Zabel

IBM Research Division, P.O. Box 218,

Yorktown Heights, NY 10598, USA

(Dated: July 7, 2003)

Abstract

Deuterium and hydrogen transport and exchange in MOS device-related stacks were studied using elastic recoil detection (ERD). The samples were typical device structures (single, double, and triple layers) alternating thermally grown silicon oxide and polysilicon, silicon nitride, silicon oxynitride, and borophosphosilicate glass (BPSG) deposited by chemical vapor (CVD) on crystalline silicon. CVD was performed with either standard (hydrogen) or deuterated precursors. Postdeposition annealings were carried out at $350-800$°C for $15-300$ min in argon or forming gas containing either D_2 or H_2. Except for silicon nitride, all materials were permeable to hydrogen and deuterium in the temperature range studied. Isotope exchange in the poly-Si/SiO_2 case was observed above 450°C. BPSG showed very little relative exchange. Concentration depth profiles for the isotopes remaining from CVD and introduced upon annealing varied with sample structure, but for a given stack were always seen to be very similar. Implications of our findings to device processing will be discussed.

PACS numbers: 66.30.-h, 61.18.Bn

Keywords: hydrogen; deuterium; Si devices; elastic recoil detection

*Present address: Department of Physics, North Carolina State University, Campus Box 8202, Raleigh, NC 27695, USA

I. INTRODUCTION

Remarkable enhancement of device reliability (lifetime) with respect to hot-electron stressing has been observed when molecular hydrogen (H_2) is replaced by deuterium (D_2) in a variety of thermal annealings of MOS structures [1–4]. The effect has been attributed to reduced hot-electron depassivation of the deuterated SiO_2/Si interface [5], where electrically active defects known as P_b centers (Si dangling bonds) can result in interface charge trap densities uncompatible with current technological needs. Despite some very encouraging reported results, like factors of $10-50$ in transistor hot-electron lifetime improvement [1], the benefit from D_2 annealings was shown inherently unstable with further wafer processing [6]. Increased annealing time and temperature (up to 5 h at 450°C) and deuterium concentration in the ambient gas (up to 100% D_2) led to up to 80-fold hot-electron lifetime improvement observed in device structures processed up to three levels on metal interconnects (M3) [7]. A finished MOS device subjected to high pressure (6 atm) annealing in 100% D_2 for 3 h at 450°C exhibited lifetime improvement by a factor of 90 [8]. At conventional processing cycles and temperatures, a deuterated nitride layer acting both as diffusion barrier and deuterium reservoir produced up to 13-fold improvement at M5 level [9, 10]. It has been found that the replacement of hydrogen with deuterium limits the deuterium incorporation at the SiO_2/Si interface [11–13], and processing with atomic deuterium has recently been suggested [14]. Possible lifetime improvement of greater than 200× has been predicted [15]. The search for optimal device manufacturing parameters continues as one tries to reach maximum advantage from the deuterium isotope effect. Relevance of transport and exchange studies to this end was soon realized.

The transport of deuterium through various transistor gate stack layers to gate dielectric interfaces was studied from deuterated forming gas annealings [4, 16]. It was found that deuterium does not seem to diffuse through undoped poly-Si in the temperature range $400-480$°C, while dopants such as boron and phosphorous greatly enhance transport of hydrogenous species. The behavior of silicon nitride layers was seen to be sensitive to prior thermal treatments; only after a high temperature annealing (>900°C) permeability was observed [4]. Borophosphosilicate glass (BPSG), metal silicides, and SiO_2 deposited from tetraethyloxysiloxane (TEOS) were shown to be permeable, just as all other materials in the device structures tested so far. Accurate quantification and profiling of hydrogen and

deuterium in such samples has proven itself challenging.

Secondary ion mass spectrometry (SIMS) has been a standard analytical technique for hydrogen and deuterium concentration depth profiling. This is understood based on the very low detection limit of SIMS, about 10^{15} cm^{-3} in the negative secondary ion mode [4], compatible with the level of dangling bonds at the nonpassivated SiO_2/Si interface (1×10^{13} cm^{-2} as measured [17] by electron paramagnetic resonance for the Si(111) substrate). Rutherford backscattering spectrometry (RBS) and elastic recoil detection (ERD) are usually employed for average film composition analysis [9, 10]. Despite analytical improvements including negative secondary ion detection and careful standard preparation, dynamic SIMS yields a relatively low accuracy (results have been quoted with 100% uncertainty) and limited depth resolution due to intermixing of material from etching ion bombardment. Most importantly, ion yields can change significantly and in a rather complex way across interfaces between different materials. In this respect, ERD has been conceived as complementary to SIMS as a profiling tool [18].

Despite significant results on the transport of hydrogenous species upon thermal annealing of MOS devices, the wide range of (mostly low if compared to the predicted maximum effect) lifetime improvements originating from deuterium application urges for a deeper understanding of the subject. The limited range of annealing times and temperatures combined with the relative complexity and diversity of the sample structures originally explored call for a systematic study of hydrogen and deuterium transport in device-like stacks. In this paper, we present such study with a materials science-oriented analysis. A wide range of materials and annealing conditions typical of semiconductor processing was used to study the thermal stability of deuterated samples and way and limitations to deuterium introduction into device structures. ERD was chosen to profile and quantify hydrogenand deuterium as an alternative to SIMS.

The paper is organized as follows: section II presents the experimental procedures used for sample preparation and analysis; results grouped by overall sample behavior in the annealing experiments are discussed in section III; section IV summarizes the work and presents conclusions.

II. EXPERIMENTAL PROCEDURE

The stacks used in this study are listed in Table I. Silicon oxide was thermally grown in dry O_2 on 200 mm Si(100) wafers. Poly-Si was deposited using standard LPCVD or RTCVD processing with SiH_4 or SiD_4 in the temperature range $\sim 600-750$°C. Silicon nitride was deposited using LPCVD ($\sim$ 700°C) or PECVD ($\sim$ 400°C). To make a 100% deuterated structure (sample DON_P), SiD_4 and ND_3 precursors were employed in the PECVD process [10, 15]. The RTP nitride sample (HON_X) was deposited on single-crystalline silicon (*c*-Si) from NH3 and SiH4 in an RTP reactor. Deposited oxynitride film has refractive index of 1.8 at 634.8 nm, from which an average composition $(SiO_2)_{0.35}(Si_3N_4)_{0.65}$ has been deduced [19, 20]. BPSG was deposited by chemical vapor deposition. Samples DOP_R and DON_P were deposited from deuterated gases; then pieces were annealed in hydrogen-containing forming gas (HFG; 90 vol.-% N_2, 10 vol.-% H_2) at $350-650$°C for $10-60$ min or in argon at $450-750$°C for the same time intervals. All other samples were deposited from hydrogenated gases; pieces were annealed in deuterium-containing forming gas (DFG) at $500-800$°C for 30 min and at 600°C for $15-300$ min. Annealings were performed in a quartz tube furnace. The samples were quickly moved to the hot zone at the annealing temperature and under H(D)FG flow. After the planned annealing time, the samples were moved to the cold zone and allowed to cool under H(D)FG flow.

Deuterium and hydrogen (hereafter designated as D and H) concentration depth profiles were determined using elastic recoil detection (ERD) [18]. In this technique, light particles ejected from the sample are detected at a forward angle. The primary beam was formed by $^{28}Si^{4+}$ ions at 9 MeV impinging at 65° relative to the sample normal. Recoil detection was performed at 85° relative to the sample normal, with coplanar incident beam, sample normal, and detector axis. A mylar foil of thickness 6.35 μm was placed in front of the detector to stop scattered ions and heavy recoils. The depth resolution of the technique is about 5 nm at sample surface and was estimated to be 10 nm at the depth of 100 nm [21]. We estimate our detection limit to be in the low-10^{13} cm^{-2} for D and H. D and H profiles were extracted from the original number of recoils *versus* recoil energy data through spectral simulations with the SIMNRA program [22]. The program allows description of the sample in terms of up to 20 layers of variable composition [23] and thickness and includes a procedure for a least-squares fitting to experimental data. Fig. 1 shows typical experimental

data and the corresponding simulated spectrum, as well as the concentration depth profile for D resulting from the fitting procedure.

In the extraction of profiles from ERD raw data, the thickness of a layer expressed in length units depends on its volumetric density; both layer thickness and extracted recoil concentration are affected by stopping powers calculated for the different materials in the sample (and foil placed in front of the detector) for ions in the primary beam and detected recoils. Fittings were performed according to the following algorithm: using available density and stopping power data, a sample structure corresponding to the nominal (*i.e.* intended from film growth or deposition) thickness of each film was assumed and simulations were run with D and H concentrations as parameters. Each film composing a stack was divided into as many layers as necessary for a good fitting, provided layer thickness was not below the estimated depth resolution of 10 nm; only for the samples having a 2 nm SiO_2 film this film was described as one single layer with the nominal thickness instead. Starting simulations with the original input structures, film thicknesses were changed upon compelling evidence from comparison to experimental data.

The stopping powers used are accurate within $10 - 20\%$ for compounds, and are much better for elemental layers [22]. We estimate that the thicknesses and concentrations presented are accurate to better than $\pm 30\%$. It should be emphasized that (i) the relative concentrations of D or H among pieces of the same sample, and (ii) the total amounts of D and H reported (areal densities) are not subject to error from densities or stopping powers [24]. Areal densities were also independently cross-checked against a standard of silicon implanted with D using integrated areas under the H and D peaks in ERD spectra. Low areal densities (and profiles with low concentration) of D are more accurate than those of H due to the absence of spectral background. Most ERD spectra showed a clear signal of H at sample surface [as in Fig. 1(a)] expected from residual hydrocarbon in the analysis chamber (kept between low-10^{-6} and mid-10^{-7} Torr) during ERD data acquisition [25]. This amounted to about 1×10^{15} cm^{-2} H and was also considered in the simulations when no clear distinction existed in ERD spectra between H originally in a sample and that introduced during analysis. The issue of ambiguity in concentration depth profile extraction from ion beam analysis has been addressed before and will not be discussed here [26, 27].

III. EXPERIMENTAL RESULTS AND DISCUSSION

A. D and H in the poly-Si/SiO_2/Si structures

Heavily doped poly-Si is used as the gate electrode material in MOS devices, as a conducting material for multilevel metallization, and as contact material for devices having shallow junctions. Dopants can be added during deposition or after, by diffusion or ion implantation. It may also be oxidized to SiO_2 in dry oxygen at $900 - 1000°C$ to form an insulator between the doped poly-Si gate and other conducting layers. As the gate electrode material, poly-Si forms the second large area interface with SiO_2 in an MOS device, adjacent to the Si channel. It is therefore important to understand to what extent and under what conditions poly-Si is permeable to hydrogen isotopes. An additional point is how much poly-Si itself is prone to isotopic exchange, since transport of hydrogenous species and reaction at the SiO_2/Si interface may also inevitably occur after the forming gas annealing, during processing steps not intended to modify the SiO_2/Si interface.

Typical profiles of D and H in sample DOP_R (see Table I) after annealings in this work are shown in Fig. 2. For the spectral simulations, we assumed the maximum D concentration in the profiles is in the ultrathin oxide film in agreement with SIMS results in the literature [4, 6, 16]. The agreement between the profiles in Fig. 2 and the nominal poly-Si layer thickness in sample DOP_R (150 nm) thus obtained is very good. The profiles indicate the presence of both D and H in very small amounts at the sample surface (< 0.1 at.-%, $< 1 \times 10^{14}$ cm^{-2}), both becoming depleted with increasing annealing temperature. Following the assumption of D peak concentration at the oxide, there is also evidence for D accumulation close to this ultrathin film, at both interfaces. H is found spread over a wider region of the sample. The bulk of poly-Si is seen to remain practically free of both isotopes, implying that interfaces with dangling bonds play a major role in D(H) accumulation. Concentration depth profiles extracted from pieces of sample DOP_R annealed in argon were very similar to their counterparts annealed in HFG.

Fig. 3 shows the areal densities of D and H close to the buried poly-Si/SiO_2/Si(100) interfaces [28] in sample DOP_R after different HFG annealings. D and H amounts are rather small, indicating less than the equivalent to one monolayer. Within the experimental range, annealing time is seen to play no significant role in D loss or H uptake. Significant D loss

starts at a temperature higher than 450°C, coinciding with the onset of H uptake. For annealings at 650°C, the longest runs lead to D concentrations below the detection limit. Concerning annealings in argon, areal densities of D were similar to those presented in Fig. 3, except that the concentrations after processing at 550°C were essentially the same as those at 450°C; at 650°C they returned to the level observed for the HFG annealings (Fig. 3). H incorporation (probably from residual H_2O and H_2 in the furnace) at levels above the detection limit happened at 550°C (two longest annealings) and at 650°C, showing no consistent dependence on time and remaining below 8×10^{13} cm^{-2}. Both D and H concentrations were below detection limit after annealings in argon at 750°C, indicating interface depassivation at this temperature consistent with previous work [35].

D and H transport has already been shown to occur for molecular and/or monatomic species in poly-Si, SiO_2, and *c*-Si [29, 30]. Therefore, D transport is expected during poly-Si deposition and both D and H transport are expected during annealing in HFG. Indications exist that transport through the substrate plays no major role in H isotope loss or uptake during annealing [21, 31]. The very low (< 0.1 at.-%) D plus H concentration found in bulk poly-Si is consistent with that previously found in device structures after annealing in D_2 following source and drain activation [4]. It is also consistent with the deep H trap concentration (below mid-10^{18} cm^{-3}) suggested for LPCVD poly-Si [29]. According to the simulations, the samples contain about 3×10^{13} cm^{-2} D plus H atoms in the ultrathin oxide films, irrespective of annealing temperature. This is three orders of magnitude higher than the expected from the solubility of D_2 in vitreous silica at 350°C and 1 atm [32]. It is in agreement with data obtained by nuclear reaction analysis for a 5.5 nm thermal SiO_2 film in which D was however incorporated from annealing at 450°C for 45 min in DFG [33].

D(H) presence in poly-Si has been connected to Si–D(H) bonds at grain boundaries [29]. Accumulation at the sample surface was attributed to the formation of D(H)-stabilized platelets. Such bonding sites are also expected wherever poly-Si and *c*-Si form interfaces with solid films. The depth resolution from ERD measurements, however, does not allow a conclusive remark about H and D accumulation close to the ultrathin SiO_2 film; we return to this point later, in the discussion of results for samples with thicker (55 nm) oxide films. O–D(H) bonds in thermal silicon oxide are present in addition to Si–D(H) [34]. Si–D bonding was hypothesized to produce D uptake at 300°C and above followed by release at 600°C, while O–D would be formed readily at 100°C and dissociated at about 800°C

[34]. Our data indicate that in the presence of H_2, the release is already active at 550°C. Absence of D (above detection limit) in the sample annealed in argon at 750°C supports findings in the literature and is consistent with the common knowledge that the SiO_2/Si interface becomes electrically depassivated after high-temperature annealings [34, 35]. For annealings in forming gas, as the H uptake exceeds the D release the former is not *only* due to exchange (although it certainly occurs). Both D and H concentrations in the samples are well above the estimated for P_b centers. Incoming H may be having access to bonding sites not passivated during poly-Si deposition. Existence of a variety of bonding sites (Si and O dangling bonds at different configurations) for H at and close to the SiO_2/Si interface has already been suggested from annealing experiments [33].

More results concerning the poly-Si/SiO_2/Si structure were obtained by studying samples HOP_R and HOP_L (see Table I). Both profiles and areal densities of D and H determined in these two samples are remarkably similar. The similarity holds not only between pieces annealed at the same temperature and for the same time, but among all annealed at up to 600°C and 300 min. Fig. 4 shows the characteristic D and H profiles for sample HOP_R under different annealing conditions. As observed for sample DOP_R (Fig. 2), small surface concentrations decrease with increasing annealing temperature. Moreover, the profiles show D and H accumulation in the region between 160 and 260 nm from the surface, which we believe corresponds to the poly-Si/SiO_2 interface and SiO_2 film, in reasonable agreement with nominal poly-Si layer thickness. Concerning the profiles shown in Fig. 2, the accumulation seen at the SiO_2/Si interface is most probably a result of enhanced diffusion through the ultrathin oxide film combined with insufficient depth resolution from the ERD measurements. Areal densities in the HOP_R and HOP_L samples were about $3-4\times10^{14}$ cm^{-2} D and 5×10^{14} cm^{-2} H for annealings at up to 600°C and 300 min and about 3×10^{14} cm^{-2} D and H for annealings at 700°C for 30 min. It should be noted that already after annealing at 500°C (the lowest annealing temperature for these samples) a significant amount of incoming D was found. No H could be detected in either sample after annealing at 800°C for 30 min, and D remained close to 1×10^{14} cm^{-2}.

The fact that samples HOP_R and HOP_L behave so similarly upon thermal annealing implies similarity between RTCVD and LPCVD poly-Si. Most of the D incorporation and H release is seen to occur at the poly-Si/SiO_2 interface and in the oxide film. The incoming isotope is seen to be closer to the sample surface in both Figs. 2 and 4. As in one case H and

in the other D is incoming, the result is not a systematic error from the ERD measurements. One feature characteristic of H and D profiles in all poly-Si/SiO_2/Si samples in this work is that only one concentration peak is seen below the sample surface. This contrasts with results from SIMS profiling of D and H in device-structures submitted to annealing at the M1 level or fully processed, which showed H and D accumulation at both oxide interfaces [36–38]. When significant exchange occurred, a factor of ~ 2 was observed between D/H concentration ratios at the poly-Si/SiO2 and SiO2/Si interfaces [37]. Such observations can be conciliated with ours if low H and D concentrations at the SiO_2/Si interface combine with significant H and D concentrations in the bulk of SiO_2, making depth resolution from ERD measurements insufficient. Our simulations indicate that this could effectively be the case. The only significant difference in sample preparation between ours and preceding experiments is the absence of metals and dopants, which are expected to generate monatomic H(D). Incorporation of D at the SiO_2/Si interface, however, does not depend on that [33, 39].

Complete exchange of D for H was achieved after annealing at 800°C. Due to low counting statistics in ERD spectra, however, D concentration depth profiles could not be extracted. Although general results have pointed out that the more D in device structures the better [7], data by different authors suggest that the actual figure of merit is the relative concentration of H isotopes at the interface [9, 15, 36, 37]. One word of caution: as stated, ERD detection limit in this work is still above the expected concentration of P_b centers at the SiO_2/Si interface. H isotope exchange at these defects, therefore, may not be complete. In fact, preliminary electrical characterization indicates a high density of interface states for the samples annealed at the highest temperature. It may well be that D is primarily bound to oxygen and, as indicated by Fig. 4, to silicon at the poly-Si/SiO_2 interface.

It should also be noted the striking difference between results for samples HOP_R and HOP_L and those for sample DOP_R. All profiles qualitatively indicate D and H bonding sites within the oxide films and close to the poly-Si/SiO_2 interface. However, areal densities at this interface differ greatly, as shown in Fig. 5. The only difference between samples DOP_R and HOP_R (besides the hydrogen isotope introduced from poly-Si deposition) is underlying oxide thickness (refer to Table I). This could explain in part the higher H concentrations in HOP_R as compared to D in DOP_R. The difference, however, does not follow the factor of 11 suggested by the oxide thicknesses. One possibility is that a significant part of the isotope from deposition could be trapped at the SiO_2 interfaces independently of film thickness.

Given that the oxide in sample DOP_R practically presents no bulk, 2×10^{14} cm^{-2} H(D) is trapped at the interfaces and a linear model suggests $< 1 \times 10^{13}$ cm^{-2} nm^{-1} H(D) in the oxide bulk. These figures are too high by one and two orders of magnitude, respectively, if again compared to those estimated in previous studies [33, 34], but experimental conditions were different and a quantitative comparison may not be valid. The fact that the ERD detection limit is reached with a 30 min annealing at 650°C for sample DOP_R and only at 800°C for sample HOP_R may be a result of the desorption kinetics; presumably all H would be gone from sample HOP_R at a lower temperature if the annealings were long enough.

Concerning the isotope introduced from the annealings, incorporation of D into HOP_R seems to be at the maximum already after 30 min at 500°C, while H seems to be continually incorporated into DOP_R between 450 and 650°C (see Fig. 5). It is not likely that a significant difference between bonding sites occurs between the samples. If uncertainties are taken into account and previous results considered, the following picture emerges. Kizilyalli et al. [7] observed increasing D uptake with increasing annealing temperature between 400 and 450°C, the same as Clark et al. [6] between 400 and 600°C. We most conclusively observe reduction of D(H) uptake at high temperatures (above 600°C). This is consistent with this being the temperature at which D(H) starts to be released from Si–D(H) bonds [34]. We therefore state that maximum incorporation occurs at temperatures close to 600°C. As the hydrogen isotopes incoming and from deposition are distinct for samples HOP_R and DOP_R, this analysis assumes that D and H have the same behavior upon thermal incorporation and desorption. The latter was predicted from first-principles calculations [40]. The fact that D(H) amounts from annealing do not follow the relationship between D(H) amounts from deposition in the samples requires further investigation, with samples of various oxide thicknesses.

We summarize our findings concerning the poly-Si/SiO_2/Si stacks as follows:

- as-deposited samples present H(D) at the surface and close to the poly-Si/SiO_2 interface, in maximum amounts respectively equal to 1 and 2×10^{14} cm^{-2};
- annealing time does not seen to play a role in H(D) loss or uptake in the $10 - 60$ min range;
- isotope incorporation from the annealing ambient starts at a temperature in the interval $450 - 500$°C;

- H isotopes from deposition and introduced upon annealing are found in the same region of the samples, with the latter slightly closer to the sample surface;
- the amount of isotope from deposition seems to depend on oxide thickness, while the amount of isotope introduced upon annealing does not ($\sim 4 \times 10^{14}$ cm^{-2});
- the isotope from deposition is continuously lost with increasing temperature, while that introduced upon annealing presents maximum concentration after annealing at 600°C;
- annealings in HFG produced release of D from deposition at above 450°C, while annealings in argon produced it just at above 550°C.

We note that these observations apply to starting structures with partially passivated SiO_2 interfaces (from the CVD process). The results imply that to take maximum advantage of the hydrogen isotope effect annealing in such cases should be performed at 600°C and that for depassivated interfaces (which is the case after source and drain activation) the annealing temperature should not be higher than that. Evidently, wafers can only be exposed to such temperature before any metallization step.

B. Silicon nitrides and oxynitride

Silicon nitride is used as a dielectric or barrier layer in the fabrication of integrated circuits. A common application is to use it as the final passivation layer (protective overcoat) of the IC. It is also applied between metal levels and on top of the silicide layer which provides contact to gate, source, and drain and as sidewall spacer in deep submicron complementary MOS technologies. In the latter case, it forms interfaces with doped Si and poly-Si. One important property of deposited Si_3N_4 is high concentration of H. Nitrogen-doped silicon oxides (silicon oxynitrides) have received attention as gate dielectrics [41]. They yield reduced boron diffusion from p^+-doped poly-Si electrodes to the Si substrate and increased hot-electron device reliability as compared to pure SiO_2.

Samples DON_P, HON_P, HBN_P, HOP_LN_P, HON_X, and HON_L (see Table I) were used to study hydrogen isotope transport and exchange in silicon nitride. Results for the first five can be grouped based on similarity. The former four samples were capped with PECVD

nitride, while HON_X had an RTP nitride. Fig. 6 shows H and D profiles in five of the nitride samples after annealing at 600°C for 300 min for comparison. Fig. 7 shows typical profiles obtained from sample HON_P. Incoming D is found at increasing depths and with somewhat increasing surface concentration with increasing annealing time and temperature. However, it could not be detected in any of the materials at the bottom of a Si_3N_4 film, restating its character of good diffusion barrier [2, 6]. Our ERD simulations indicate H depletion at the sample surface and close to the Si_3N_4/SiO_2 interface, which however could be an artifact mainly from superestimation of experimental energy resolution. The result at the sample surface has been hypothesized before [21]. Qualitatively, the profile of H remaining from the CVD process does not change with annealing conditions. The profiles also show D and H concentrations characteristic of silicon nitride produced by PECVD, much higher than those found in poly-Si and SiO_2.

Fig. 8 shows H and D areal densities in samples DON_P and HON_P as a function of temperature for 30 min annealings. For the isotope remaining from CVD, the results are two orders of magnitude higher than those found for the poly-Si samples. Continuous release occurs with increasing temperature, with no significant effect of anealing time (not shown) or underlying oxide thickness. This indicates that in order to function as D reservoir the PECVD nitride has to be annealed at above 500°C. Sample HON_P still shows a high concentration of H after annealing at 800°C, also contrasting with the results observed for poly-$Si/SiO_2/Si$ stacks. D or H incorporation from the annealing step is also continuous and much higher than that observed before. A large difference between hydrogen isotope release and uptake evidences a competition between exchange and other processes.

Sample HON_L presented D and H profiles qualitatively similar to those in samples DON_P, HON_P, HBN_P, and HOP_LN_P (Fig. 6). However, H concentrations were much lower ($\leq$ 5 at.%), as expected for silicon nitride produced by LPCVD (and therefore, at higher temperature as compared to PECVD). H release and D uptake also followed the general trend observed in Fig. 8. Interestingly, D uptake occured at the same level observed for PECVD nitrides, *i.e.* with a maximum of close to 1×10^{16} cm^{-2} after annealing at 800°C for 30 min, which in this case represents about 80% of the original H areal density. Moreover, the sum of H and D amounts was seen to remain constant in the experimental range of annealing times and temperatures, meaning that isotopic exchange was practically the only process taking place. If bonding sites for D are of the same nature in PECVD and LPCVD

silicon nitride, this essentially suggests that the former presents a high density of defects whose configurations favor the process competing with exchange.

The dynamics of D and H in PECVD and LPCVD silicon (oxy)nitrides upon thermal annealing was studied in detail by Arnoldbik et al. [21, 42]. One significant difference between the nitrides and poly-Si/SiO_2/Si stacks is the existence of N–H(D) bonds, which were shown to hold 1/4 of all H(D) in PECVD nitride [42]. It is a strong bond (4.69 eV in NH_3 [43]), accounting for the increasing incorporation of D(H) with increasing annealing temperature. To a significant extent, H and D areal densities observed here in PECVD and LPCVD silicon nitrides agree with published data [21, 42]. Net reduction in D plus H content upon thermal annealing was attributed to the cross-linking reaction:

$$\equiv\text{Si–H} + =\text{N–H} \longrightarrow \equiv\text{Si–N}= + \text{H}_2 \tag{1}$$

starting at 600°C. This should be the process competing with exchange suggested by our data for PECVD nitrides; it is apparently suppressed in the LPCVD sample. Beyond the general agreement, we also find a number of significant differences relative to previously reported results. Thick (1000 nm) PECVD nitrided films were seen [42] to crack upon annealings in 4 vol.-% D_2 in N_2 between 800 and 1000°C, with D incorporation at both sample surface and interface between nitride and substrate. Chen and Wallace [4] also observed D transport, now through a LPCVD silicon nitride film and after a > 900°C annealing step. We did not observe cracking nor permeation to D in the temperature range $350 - 800$°C. D incorporation into LPCVD nitrides [21] at the annealing conditions reported above (4 vol.-% D_2 in N_2, $800 - 1000$°C) was seen to obey a linear relationship with the square root of time, characterizing a Fickian diffusion process. We could not consistently observe such behavior, since as commented annealing time had no significant effect on D uptake. Arrhenius plots of the D uptake did not show straight lines either, preventing us from deriving a single activation energy. Both observations could be due to the different annealing temperature ranges in this and previous studies. The temperature range in our experiments includes the expected transition between active and inactive trapping in Si–H(D) bonds besides of N–H(D) (which could also appear in a variety of different energy configurations) and this could be at the bottom of our observations. Concerning annealings in argon, the DON_P sample yielded practically the same D loss as in HFG after a given annealing time at the same temperature. In this case, some H incorporation was also observed after the

annealings in argon, in amounts increasing with temperature, probably from contamination of the ambient gas with H_2 or H_2O.

Sample HOX, a silicon oxynitride, showed a distinctive behavior upon annealing in DFG. Fig. 9 shows D and H profiles obtained after DFG annealings at the given conditions. Profiles in the sample annealed at 600°C are characteristic of all annealings up to 300 min at this temperature; the D profile observed after treatment at 700°C qualitatively applies to 800°C. D and H are seen to occupy essentially the same region of the samples. The profiles also indicate little or no incorporation of D into the oxide underlying the oxynitride film. This includes the sample annealed at 800°C, in which the incoming isotope could not be profiled in the case of poly-Si/SiO_2. Fig. 10 shows D and H areal densities in sample HOX after the annealings. Absolute numbers ($1.2 - 0.1 \times 10^{16}$ cm^{-2} for D, 6×10^{15} cm^{-2} to below detection limit for H) are in-between those observed in poly-Si/SiO_2/Si and in the nitrides. The relationship between incoming D and H remaining from deposition is similar to the one in Fig 5, obtained for the poly-Si/SiO_2/Si samples. Already after 30 min at 500°C the amount of incoming D is higher than that of remaining H. Incoming D is found at maximum areal density after 30 min at 600°C. After annealing at 800°C D is found in lower amount, but in the absence of H. Results in the literature [21, 42] indicate for oxynitrides relative to nitrides less H from the deposition, higher D uptake, and lower H loss. We confirm all these observations. However, in our case D incorporation did not increase monotonically with increasing annealing temperature, as observed here for the nitrides and previously for oxynitrides in the range 800−1000°C. We believe this is due to significant Si–H concentration from deposition, which together with N–H would respond for the decrease in bonding sites for D according to Eq. 1. Previously, Si–H bonds were found in only minor concentration in silicon oxynitride [42].

We summarize our findings concerning the stacks capped with silicon nitride as follows:

- as-deposited samples show H(D) evenly distributed, except for depletion at the sample surface, in amounts expected from the CVD processes ($5 - 15$ at.-%, mid- to low-10^{16} cm^{-2} for 50 nm films);

- annealing time does not show significant effect on H(D) loss or uptake in the 15−60 min range, but it does in going from 60 to 300 min, resulting in increased loss of the isotope from deposition and uptake of the isotope from annealing;

- isotope incorporation from the annealing ambient starts at above 450°C;
- the isotope from deposition is evenly lost along the nitride films with increasing annealing temperature, starting at above 500°C;
- the isotope introduced upon annealing is found deeper and in increasing amounts with increasing annealing temperature;
- specifically for PECVD nitride, thermally activated cross-linking significantly reduces the number of bonding sites for H(D);
- annealings in argon or in HFG, other conditions being equal, produced practically the same D loss.

Based on these observations, we conclude that the best use for silicon nitride concerning the hydrogen isotope effect is as both a barrier to the transport of hydrogenous species and D reservoir. Noting that it contains a significant amount of the H isotope in the precursor gases and having in sight the possible effect of further processing on a SiO_2/Si interface passivated with D, we believe it should be deposited from deuterated gases, following the approach of Clark et al. [10, 15]. Significant amount of D still remains in the film after annealings at ~ 600°C.

C. Borophosphosilicate glass

BPSG is formed by doping silica with boron and phosphorous. Thin BPSG films are widely used in IC manufacturing as dielectrics between metal interconnections and underlying structures, as passivation and planarization layers, and as traps (getters) for mobile alkali cations. One of the most important properties of BPSG is reflow (fusion) temperature, which can be tailored to the demands of a given application by varying the amounts of dopants incorporated to the silicon dioxide matrix.

Fig. 11 shows D and H profiles in sample HB after annealing in DFG for 30 min at different temperatures. H from deposition is seen to be evenly distributed in concentrations close to 8 at.-%, except for depletion at the surface and interface with *c*-Si. D from annealing seems to be stabilized far from the sample surface. Its maximum concentration is below 0.5 at.-%. The disagreement between nominal film thickness and that extracted from the ERD profiles

should be due to inaccuracy in stopping power and/or density estimation for this rather complex material. The profiles suggest loss of both D and H with increasing annealing temperature. Fig. 12 shows H and D amounts in sample HB after different annealings. H areal densities in the BPSG film are significant — close to those found in PECVD silicon nitride films of roughly half thickness. For the annealing conditions tested, they apparently show one significant transition, when annealing is extended from 60 to 300 min at 600°C. D areal density show a maximum after the mildest condition tested, 30 min at 500°C. Although the absolute result is quite high (1.7×10^{15} cm^{-2}), it represents less than 5% of the H amount in the same sample. D amounts are seen to decrease with annealing time and temperature, until practically reaching the ERD detection limit after 30 min at 800°C.

Analysis of data for sample HON$_{\rm P}$B is instructive for combining basic features attributed to BPSG with those of a PECVD nitride. Fig. 13 shows D and H profiles in sample HON$_{\rm P}$B after annealing in DFG at the given conditions. Qualitatively, the profile shown for after 60 min at 600°C describes all samples annealed at up to this time and temperature; that shown for after 30 min at 700°C also applies to 300 min at 600°C and 30 min at 800°C. We presume the step in the concentration depth profiles at the depth of 75 nm signals the interface between BPSG and Si_3N_4. This result is within 25% of the nominal BPSG film thickness, and, therefore, within the estimated accuracy of our profiling technique. D is found mainly at the interface and extending into the nitride, whereas H is present throughout the BPSG layer, in the nitride, and apparently in the underlying SiO_2. The profiles indicate D at a somewhat lower concentration than in the uncapped nitrides subjected to equivalent annealings. H is present at a significant concentration in BPSG and at a higher level in the nitride, in reasonable agreement with Fig. 7(b). Both results for D and H in BPSG are consistent with Figs. 11 and 12. Fig. 14 shows D and H amounts in sample HON$_{\rm P}$B after annealing. H amounts are very high, as expected from the profiles, and decrease with increasing annealing temperature. Such decrease was seen to be characteristic of the nitrides (Fig. 8) and also of the BPSG single layer, specifically in going from 60 min to 300 min at 600°C. The amounts of D incorporated are similar to those found in the nitrides, but a unique feature of sample HON$_{\rm P}$B is a minimum in D incorporation between the extreme annealing temperatures. Data for the single BPSG layer (Fig. 12) indicate monotonically decreasing D amounts for increasing annealing time and temperature, which combined with the continuous increase expected for the underlying nitride layer in sample HON$_{\rm P}$B produce

the observed result.

Our results most clearly restate the permeability of BPSG to D and H [4]. Its rather high efficiency in transporting hydrogenous species (as stated by the level of D incorporation at and H loss from the underlying nitride) should be related to the presence of boron and phosphorous, as originally done in connection to data for doped poly-Si [4]. The decreasing D uptake with increasing annealing temperature is consistent with relatively weak B–D(H) and P–D(H) bonding, high thermal budgets leading to depassivation rather than exchange. The high H amount in BPSG doubtlessly not prone to exchange remains to be explained.

Our annealing experiments with BPSG films indicate that:

- as-deposited samples present H concentration close to 8 at.-%, evenly distributed except for depletion at the surface and interface with *c*-Si;
- H loss is expressive only in going from 60 to 300 min at 600°C;
- D uptake is maximum at or below 30 min at 500°C;
- BPSG is quite efficient in transporting D(H) to underlying films;
- BPSG is very little prone to isotope exchange.

It should be noted that the physical properties of BPSG greatly depend on boron and phosphorous doping, which vary significantly depending on its application. Given the observations above, we believe that BPSG should be separated from the SiO_2/Si interface by a barrier to the transport of hydrogenous species if increased benefit is to be obtained from the hydrogen isotope effect.

IV. SUMMARY AND CONCLUSIONS

We have studied D and H transport and exchange upon thermal annealing in typical MOS device structures in the ranges $10 - 300$ min and $350 - 800$°C using ERD. Our results indicate advantage in comparison to SIMS in the accuracy with which D and H amounts were determined; concentration depth profiling was limited by depth resolution. Poly-Si/SiO_2/Si, silicon nitrides, silicon oxynitride, and BPSG layers and stacks were investigated. Our results clearly show that poly-Si and BPSG are effective in transporting hydrogenous species at

rather low temperatures. Silicon nitrides, on the other hand, are good barriers, even at relatively high temperatures. This barrier, however, can be overcome depending on nitride thickness and annealing time and temperature. Deposition of poly-Si from a deuterated source does not seem to be a key element.

V. ACKNOWLEDGMENT

The authors wish to thank J. L. Speidell and S. A. Cordes from IBM Research Division at Yorktown Heights for providing the facilities for sample annealing, D. C. Mosher and M. B. Rice from IBM Microelectronics Division at Burlington for the deposition of nitride and poly-Si films, and Z. J. Luo from Yale University for useful discussions.

[1] J. W. Lyding, K. Hess, and I. C. Kizilyalli, Appl. Phys. Lett. **68**, 2526 (1996).

[2] I. C. Kizilyalli, J. W. Lyding, and K. Hess, IEEE Electron Device Lett. **18**, 81 (1997).

[3] H. C. Mogul, L. Cong, R. M. Wallace, P. J. Chen, T. A. Rost, and K. Harvey, Appl. Phys. Lett. **72**, 1721 (1998).

[4] P. J. Chen and R. M. Wallace, J. Appl. Phys. **86**, 2237 (1999).

[5] K. Hess, I. C. Kizilyalli, and J. W. Lyding, IEEE Trans. Electron Devices **45**, 406 (1998).

[6] W. F. Clark, T. G. Ference, T. B. Hook, K. M. Watson, S. W. Mittl, and J. S. Burnham, IEEE Electron Device Lett. **20**, 48 (1999).

[7] I. C. Kizilyalli, G. C. Abeln, Z. Chen, J. Lee, G. Weber, B. Kotzias, S. Chetlur, J. W. Lyding, and K. Hess, IEEE Electron Device Lett. **19**, 444 (1998).

[8] R. A. B. Devine, J. L. Autran, W. L. Warren, K. L. Vanheusdan, and J. C. Rostaing, Appl. Phys. Lett. **70**, 2999 (1997).

[9] T. G. Ference, J. S. Burnham, W. F. Clark, T. B. Hook, S. W. Mittl, M. W. Kimball, and L.-K. K. Han, IEEE Trans. Electron Devices **46**, 747 (1999).

[10] W. F. Clark, T. G. Ference, S. W. Mittl, J. S. Burnham, and E. D. Adams, IEEE Electron Device Lett. **20**, 501 (1999).

[11] K. Cheng, K. Hess, and J. W. Lyding, IEEE Electron Device Lett. **22**, 441 (2001).

[12] K. Cheng, K. Hess, and J. W. Lyding, J. Appl. Phys. **90**, 6536 (2001).

[13] K. Cheng, J. Lee, and J. W. Lyding, Appl. Phys. Lett. **77**, 2358 (2000).

[14] M. C. Hersam, N. P. Guisinger, J. Lee, K. Cheong, and J. W. Lyding, Appl. Phys. Lett. **80**, 201 (2002).

[15] W. F. Clark, P. E. Cottrell, T. G. Ference, S.-H. Lo, J. G. Massey, S. W. Mittl, and J. H. Rankin, Channel hot-electron and hot-hole improvement in Al and Cu multilevel metal CMOS using deuterated anneals and passivating films, Washington, DC, IEDM 1999, pp. 4.3.1 – 4.3.4.

[16] P. J. Chen and R. M. Wallace, Appl. Phys. Lett. **73**, 3441 (1998).

[17] A. Stesmans and G. Van Gorp, Appl. Phys. Lett. **57**, 2663 (1990).

[18] W. M. Arnold Bik and F. H. P. M. Habraken, Rep. Prog. Phys. **56**, 859 (1993).

[19] S. V. Hattangady, H. Niimi, and G. Lucovsky, J. Vac. Sci. Technol. A **14**, 3017 (1996).

[20] D. M. Brown, P. V. Gray, F. K. Heumann, H. R. Philipp, and E. A. Taft, J. Electrochem.

Soc. **115**, 311 (1968).

[21] W. M. Arnoldbik, C. H. M. Marée, A. J. H. Maas, M. J. van den Boogaard, F. H. P. M. Habraken, and A. E. T. Kuiper, Phys. Rev. B **48**, 5444 (1993).

[22] M. Mayer, *SIMNRA User's Guide*, Max-Planck-Institut für Plasmaphysik, Garching, Germany, 1997, Technical Report IPP 9/113.

[23] Composition is variable in the sense that, just as thickness, it is a fitting parameter. Within a layer, elemental concentrations are constant, so that extracted profiles are not smooth, but a sequence of steps as shown for D in Fig. 1(b). From that plot it can be inferred that the sample was described as a superposition of 9 layers.

[24] Strictly, poor estimation of stopping powers can lead to error in the determination of areal densities. In this work, however, the maximum relative error of this origin is estimated to be less than 0.5%.

[25] M. J. F. Healy, Nucl. Instr. and Meth. B **129**, 130 (1997).

[26] P. F. A. Alkemade, F. H. P. M. Habraken, and W. F. Van der Weg, Nucl. Instr. and Meth. B **45**, 139 (1990).

[27] J. W. Butler, Nucl. Instr. and Meth. B **45**, 160 (1990).

[28] Areal densities in the plot correspond to H and D beyond 105 nm in the profiles of Fig. 2.

[29] N. H. Nickel, W. B. Jackson, and J. Walker, Phys. Rev. B **53**, 7750 (1996).

[30] N. H. Nickel, W. B. Jackson, I. W. Wu, C. C. Tsai, and A. Chiang, Phys. Rev. B **52**, 7791 (1995).

[31] G. Schols and H. E. Maes, High-temperature hydrogen anneal of MNOS structures, San Francisco, CA, Symposium on Silicon Nitride Thin Insulating Films 1983, pp. 94 – 110.

[32] J. E. Shelby, J. Appl. Phys. **48**, 3387 (1977).

[33] I. J. R. Baumvol, E. P. Gusev, F. C. Stedile, F. L. Freire, Jr., M. L. Green, and D. Brasen, Appl. Phys. Lett. **72**, 450 (1998).

[34] S. M. Myers, J. Appl. Phys. **61**, 5428 (1987).

[35] K. L. Brower, Phys. Rev. B **38**, 9657 (1988).

[36] J. Lee, Z. Chen, K. Hess, and J. W. Lyding, Deuterium sintering of CMOS technology for improved hot carrier reliability, San Francisco, CA, Defect and Impurity Engineered Semiconductors and Devices 1998, pp. 301 – 312.

[37] J. Lee, S. Aur, R. Eklund, K. Hess, and J. W. Lyding, J. Vac. Sci. Technol. A **16**, 1762 (1998).

[38] J. Lee, J. E. Baker, R. G. Wilson, and J. W. Lyding, SIMS depth profiles of ^{1}H and ^{2}H at the SiO_2/Si interface of deuterium-sintered CMOS devices, Orlando, FL, SIMS XI 1997, pp. 205–208.

[39] K. Muraoka, S. Takagi, and A. Toriumi, Evidence for asymmetrical hydrogen profile in thin D_2O oxidized SiO_2 by SIMS and modified TDS, Osaka, Japan, International Conference on Solid State Devices and Materials 1996, pp. 205 – 208.

[40] C. G. Van de Walle, J. Vac. Sci. Technol. A **16**, 1767 (1998).

[41] E. P. Gusev, H.-C. Lu, E. L. Garfunkel, T. Gustafsson, and M. L. Green, IBM J. Res. Develop. **43**, 265 (1999).

[42] W. M. Arnoldbik, C. H. M. Marée, and F. H. P. M. Habraken, Appl. Surf. Sci. **74**, 103 (1994).

[43] *CRC Handbook of Chemistry and Physics*, 81st ed., edited by D. R. Lide (CRC, Boca Raton, 2000).

LIST OF TABLES

TABLE I: Sample identification and nominal structure (*i.e.* intended from film growth or deposition).

	Nominal sample structure (on Si substrate)		
Sample[a]	Base film	Film 2	Film 3
DOP_R	2 nm SiO_2	150 nm RTCVD poly-Si	—
DON_P	2 nm SiO_2	50 nm PECVD Si_3N_4	—
HOP_R	55 nm SiO_2	200 nm RTCVD poly-Si	—
HOP_L	55 nm SiO_2	200 nm LPCVD poly-Si	—
HOP_LN_P	55 nm SiO_2	200 nm LPCVD poly-Si	50 nm PECVD Si_3N_4
HON_P	55 nm SiO_2	50 nm PECVD Si_3N_4	—
HON_L	55 nm SiO_2	50 nm LPCVD Si_3N_4	—
HON_X	55 nm SiO_2	50 nm RTP Si_3N_4	—
HON_PB	55 nm SiO_2	50 nm PECVD Si_3N_4	100 nm BPSG
HOX	55 nm SiO_2	50 nm RTCVD Si_3ON_3	—
HB	100 nm BPSG	—	—
HBN_P	100 nm BPSG	50 nm PECVD Si_3N_4	—

[a]Samples have been coded using the following convention: D or H stand for the isotope from deposition (*i.e.* in the CVD precursors); O stands for oxide, P for poly-Si, N for nitride, X for oxynitride, and B for BPSG; Indices denote deposition process: R for RTCVD, P for PECVD, L for LPCVD, and X for RTP. For example, DOP_R is a stack of silicon oxide and poly-Si on Si, in which the poly-Si was deposited by RTCVD using SiD_4 as precursor.

FIGURE CAPTIONS

FIG. 1: (a) Experimental (data points) and simulated (line) ERD spectrum for a sample of a H isotope exchange experiment (the arrows indicate the position in the recoil spectrum corresponding to the indicated isotope at the sample surface); (b) D concentration depth profile producing the high-energy region (above 0.8 MeV) of the simulated curve.

FIG. 2: (a) D and (b) H concentration depth profiles in sample DOP_R after 30 min annealings in HFG at the temperatures indicated. The results are estimated to be accurate to better than $\pm 30\%$ in both concentration and depth scales. In this and forthcoming profile plots, the nominal sample structure is indicated with the sample label; marks at the top axis indicate the location of interfaces as extracted from ERD simulations.

FIG. 3: D and H areal densities beyond 105 nm in sample DOP_R as a function of annealing temperature in HFG with annealing time as parameter. The error bar (1σ) shown for D also applies to H and refers only to the analytical procedure.

FIG. 4: (a) D and (b) H concentration depth profiles in sample HOP_R after 30 min annealings in DFG at the temperatures indicated.

FIG. 5: D and H areal densities in samples DOP_R (beyond 105 nm) and HOP_R (beyond 130 nm) as a function of annealing temperature after 30 min annealings in HFG and DFG, respectively.

FIG. 6: (a) D and (b) H concentration depth profiles in various nitride samples after 300 min annealings in DFG at 600°C.

FIG. 7: (a) D and (b) H concentration depth profiles in sample HON_P after 30 min annealings in DFG at the temperatures indicated.

FIG. 8: D and H areal densities in samples DON_P and HON_P as a function of annealing temperature after 30 min annealings in HFG and DFG, respectively.

FIG. 9: (a) D and (b) H concentration depth profiles in sample HOX after annealings in DFG at the temperatures and for the times indicated.

FIG. 10: D, H, and D plus H areal densities in sample HOX after annealings in DFG at the temperatures and for the times indicated.

FIG. 11: (a) D and (b) H concentration depth profiles in sample HB after annealings in DFG at the temperatures and for the times indicated.

FIG. 12: D, H, and D plus H areal densities in sample HB after annealings in DFG at the temperatures and for the times indicated.

FIG. 13: (a) D and (b) H concentration depth profiles in sample HON_PB after annealings in DFG at the temperatures and for the times indicated.

FIG. 14: D, H, and D plus H areal densities in sample HON_PB after annealings in DFG at the temperatures and for the times indicated.

Krug et. al., Fig. 1

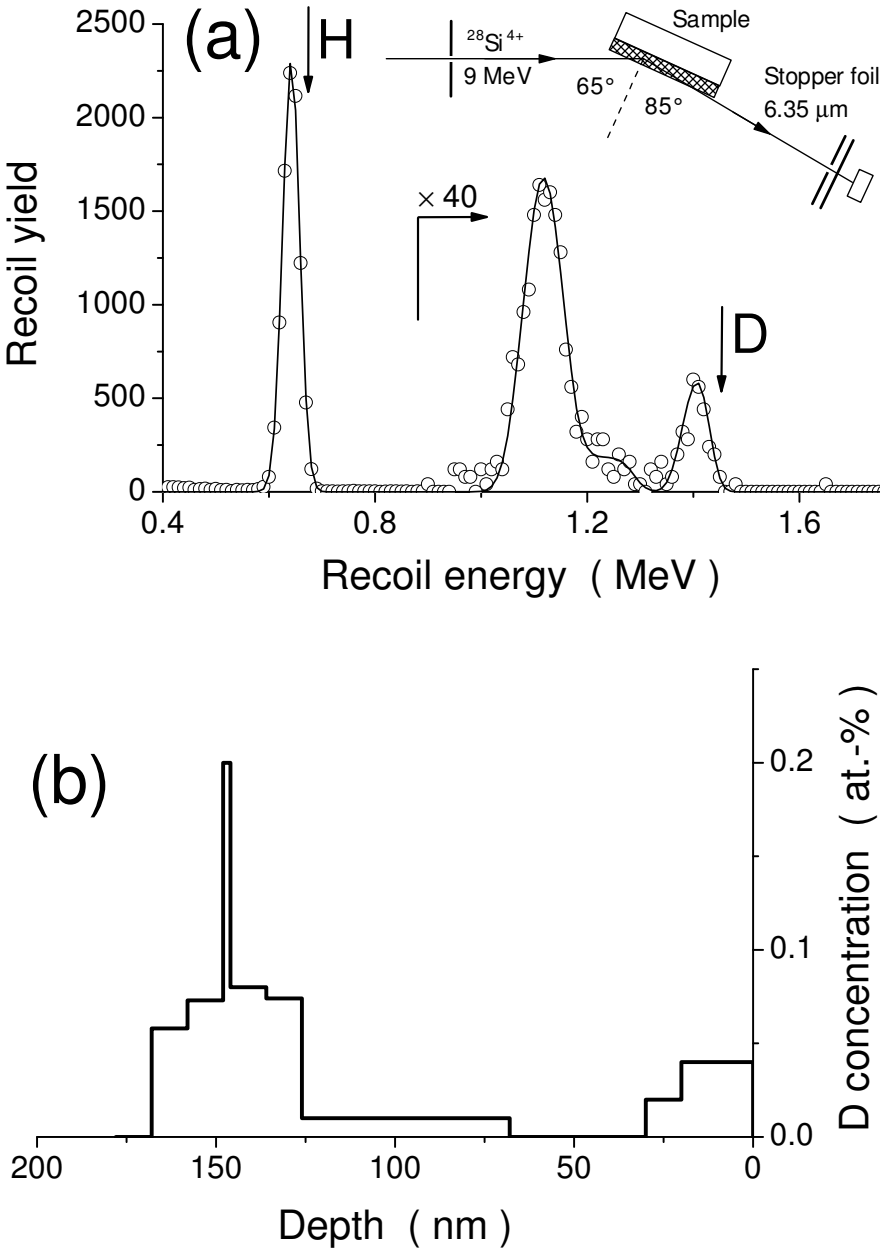

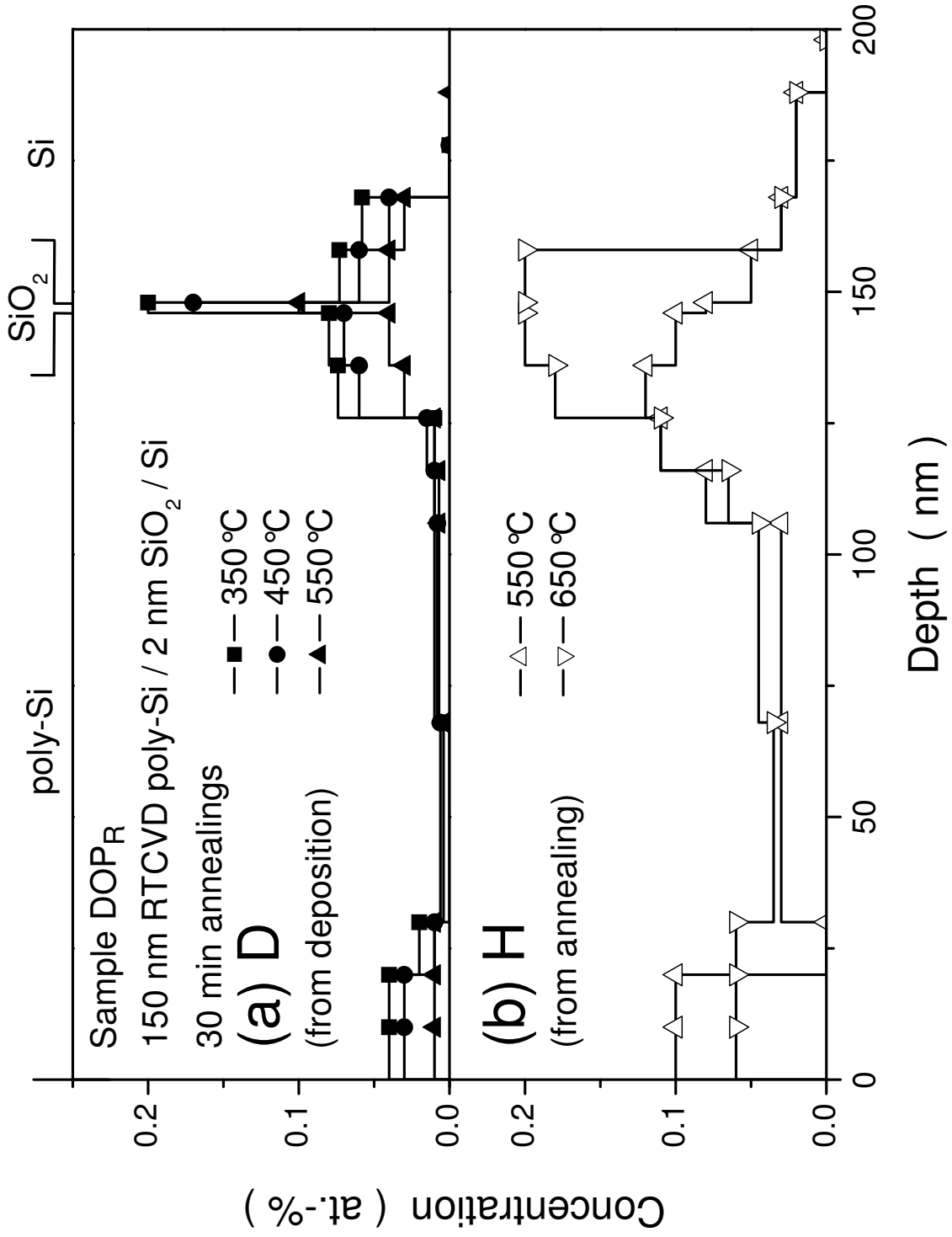
poly-Si
SiO2
Si
Sample DOPR
150 nm RTCVD poly-Si / 2 nm SiO2 / Si
30 min annealings
(a) D
(from deposition)
350 °C
450 °C
550 °C
(b) H
(from annealing)
550 °C
650 °C
Concentration (at.-%)
Depth (nm)
0.0
0.1
0.2
0
50
100
150
200

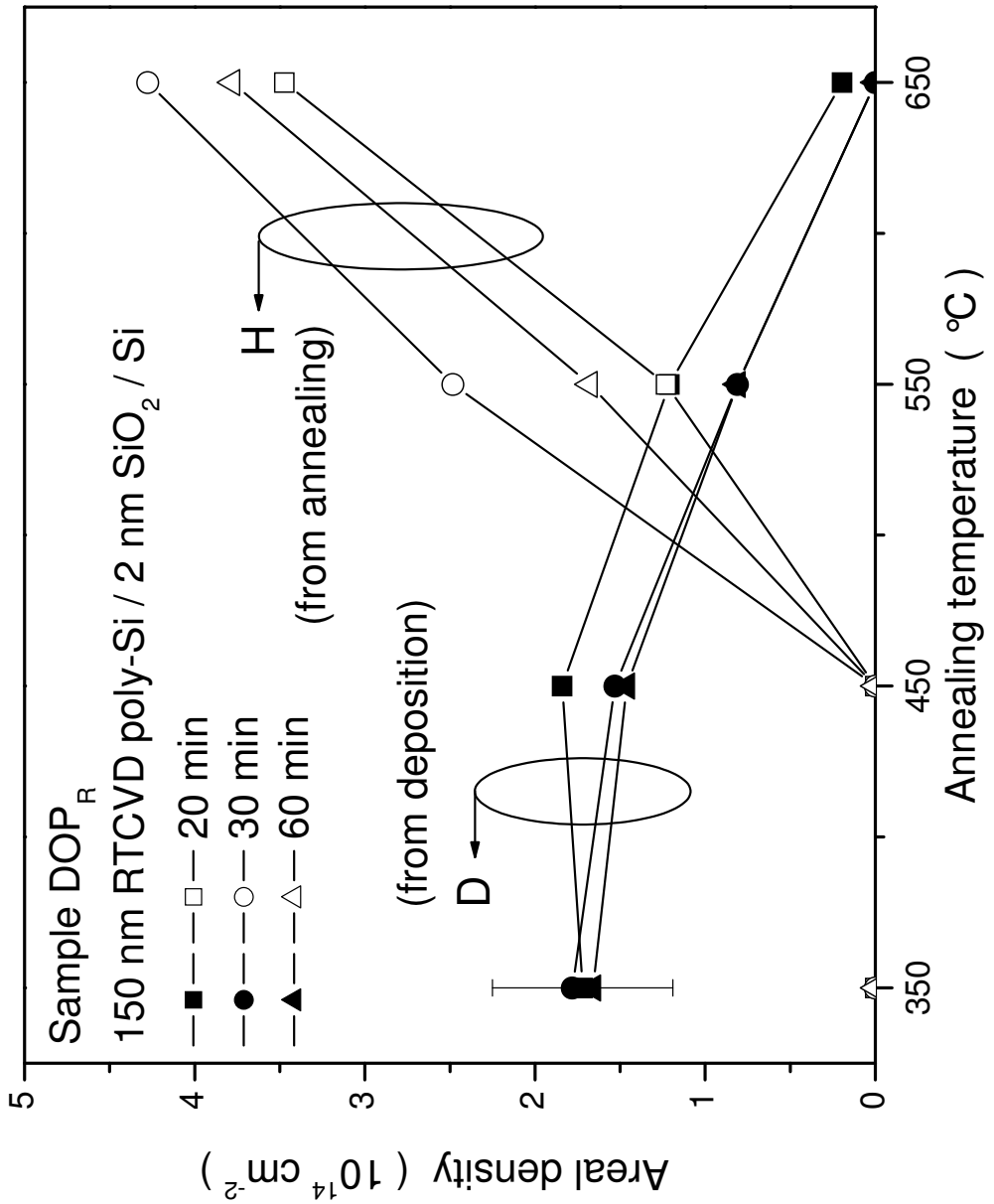
Sample DOP$_R$
150 nm RTCVD poly-Si / 2 nm SiO$_2$ / Si
20 min
30 min
60 min
H
(from annealing)
D
(from deposition)
Areal density (10^{14} cm^{-2})
Annealing temperature (°C)
0
1
2
3
4
5
350
450
550
650

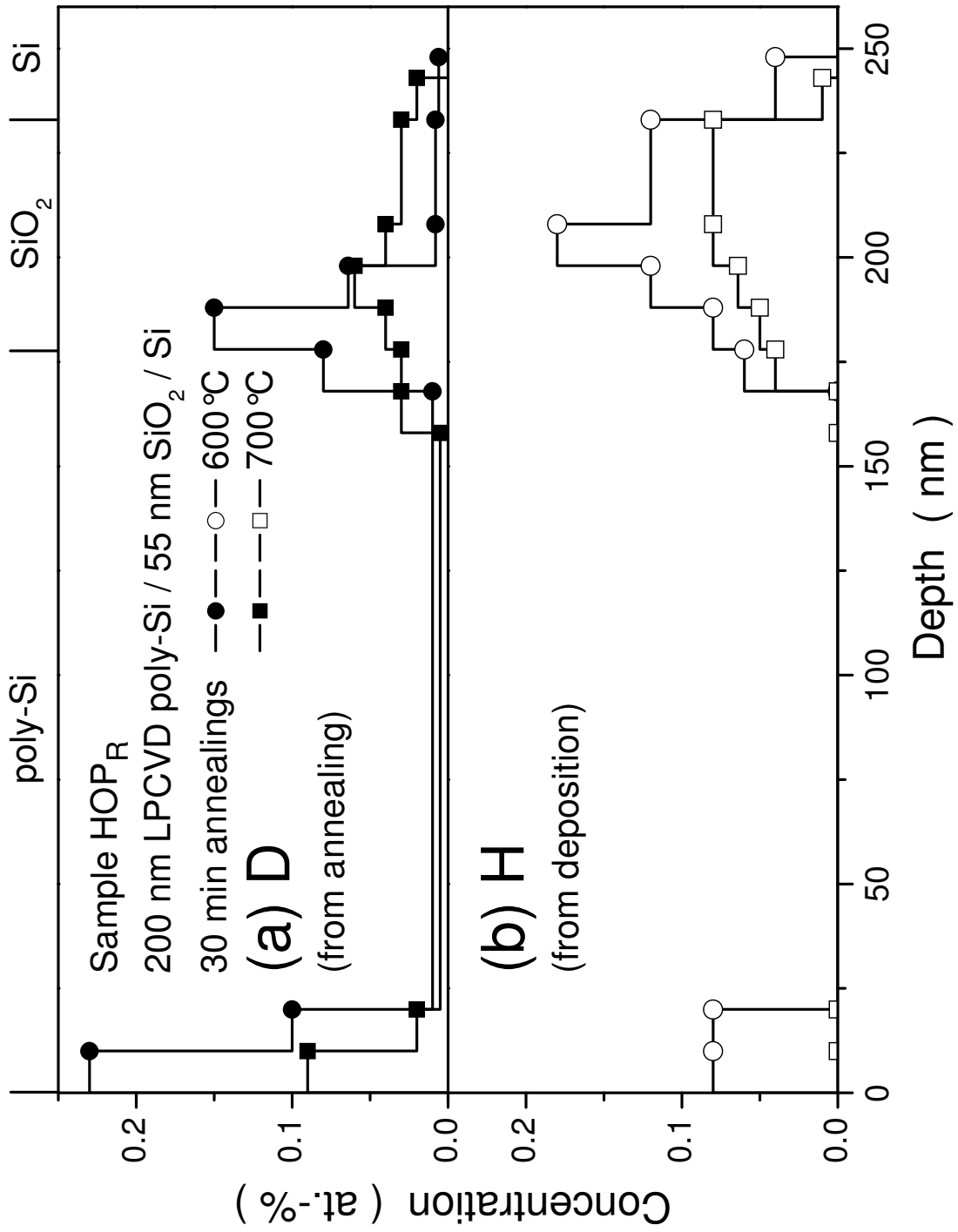
poly-Si
SiO2
Si
Sample HOPR
200 nm LPCVD poly-Si / 55 nm SiO2 / Si
30 min annealings
600 °C
700 °C
(a) D
(from annealing)
(b) H
(from deposition)
Concentration (at.-%)
Depth (nm)
0.2
0.1
0.0
0.2
0.1
0.0
0
50
100
150
200
250

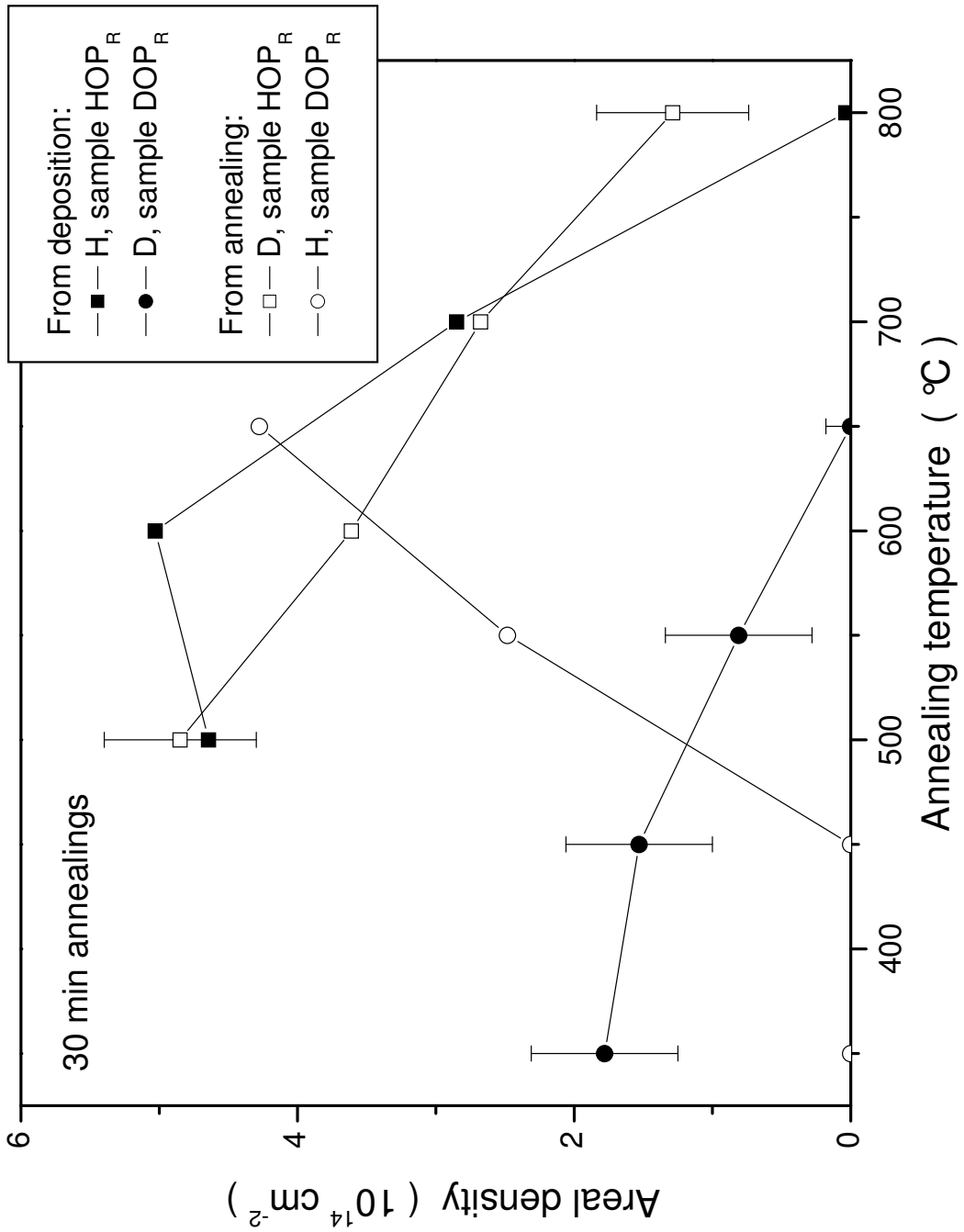
From deposition:
H, sample HOP$_R$
D, sample DOP$_R$
From annealing:
D, sample HOP$_R$
H, sample DOP$_R$
30 min annealings
Areal density (10^{14} cm^{-2})
Annealing temperature (°C)
0
2
4
6
400
500
600
700
800

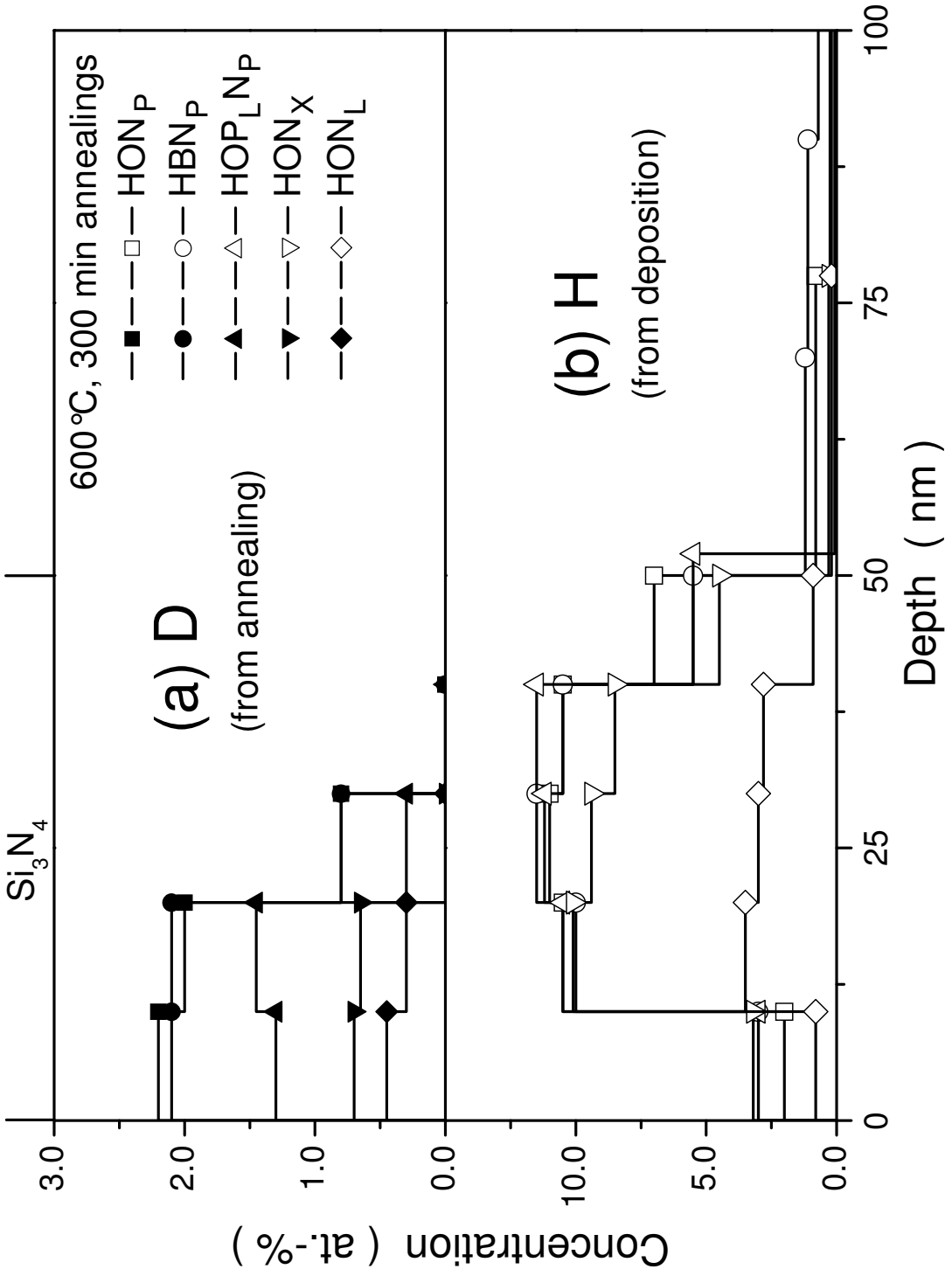
Si3N4
600 °C, 300 min annealings
HONP
HBNP
HOPLNP
HONX
HONL
(a) D
(from annealing)
(b) H
(from deposition)
Concentration (at.-%)
Depth (nm)
3.0
2.0
1.0
0.0
10.0
5.0
0.0
0
25
50
75
100

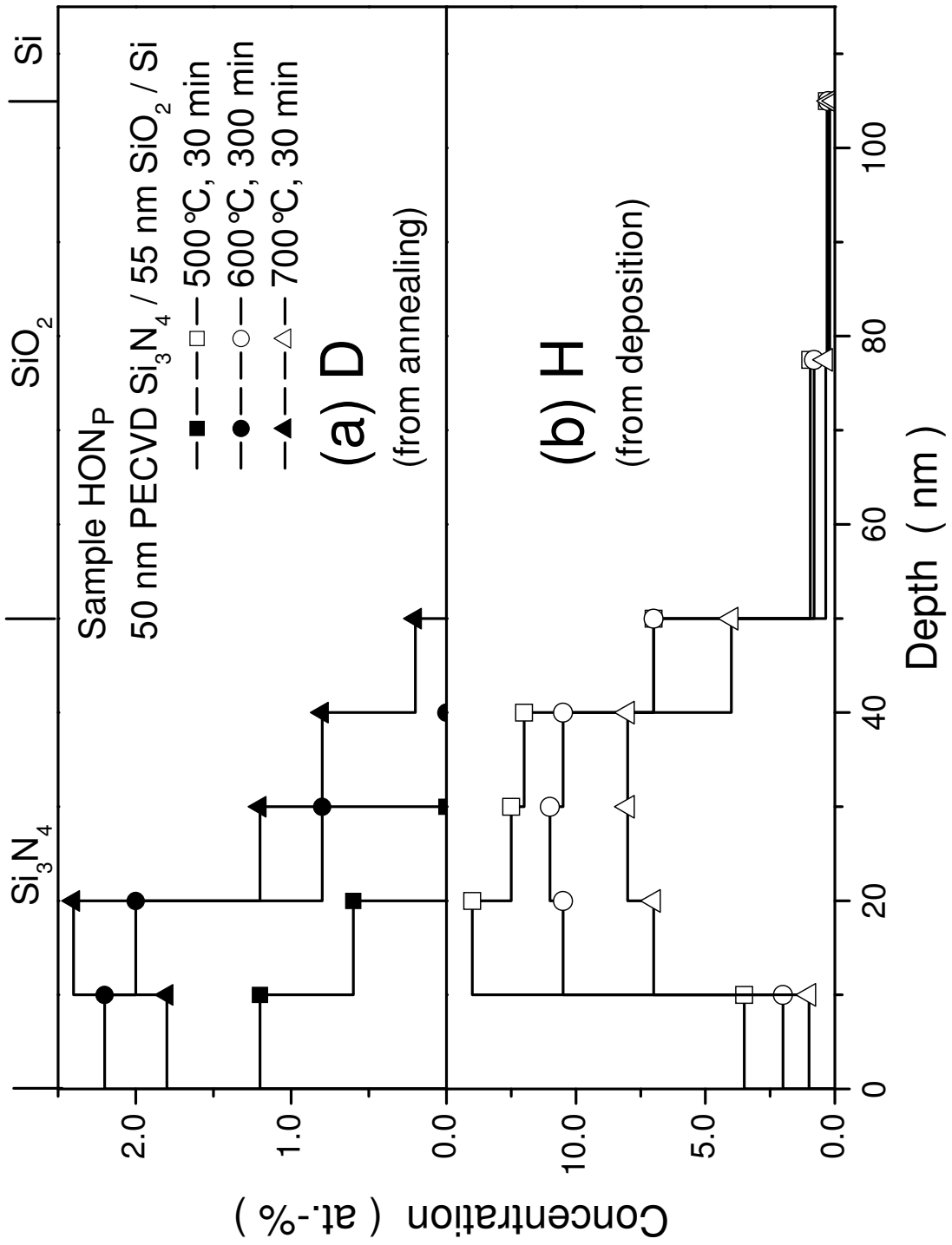
Si
SiO2
Si3N4
Sample HONP
50 nm PECVD Si3N4 / 55 nm SiO2 / Si
500 °C, 30 min
600 °C, 300 min
700 °C, 30 min
(a) D
(from annealing)
(b) H
(from deposition)
Concentration (at.-%)
Depth (nm)
2.0
1.0
0.0
10.0
5.0
0.0
0
20
40
60
80
100

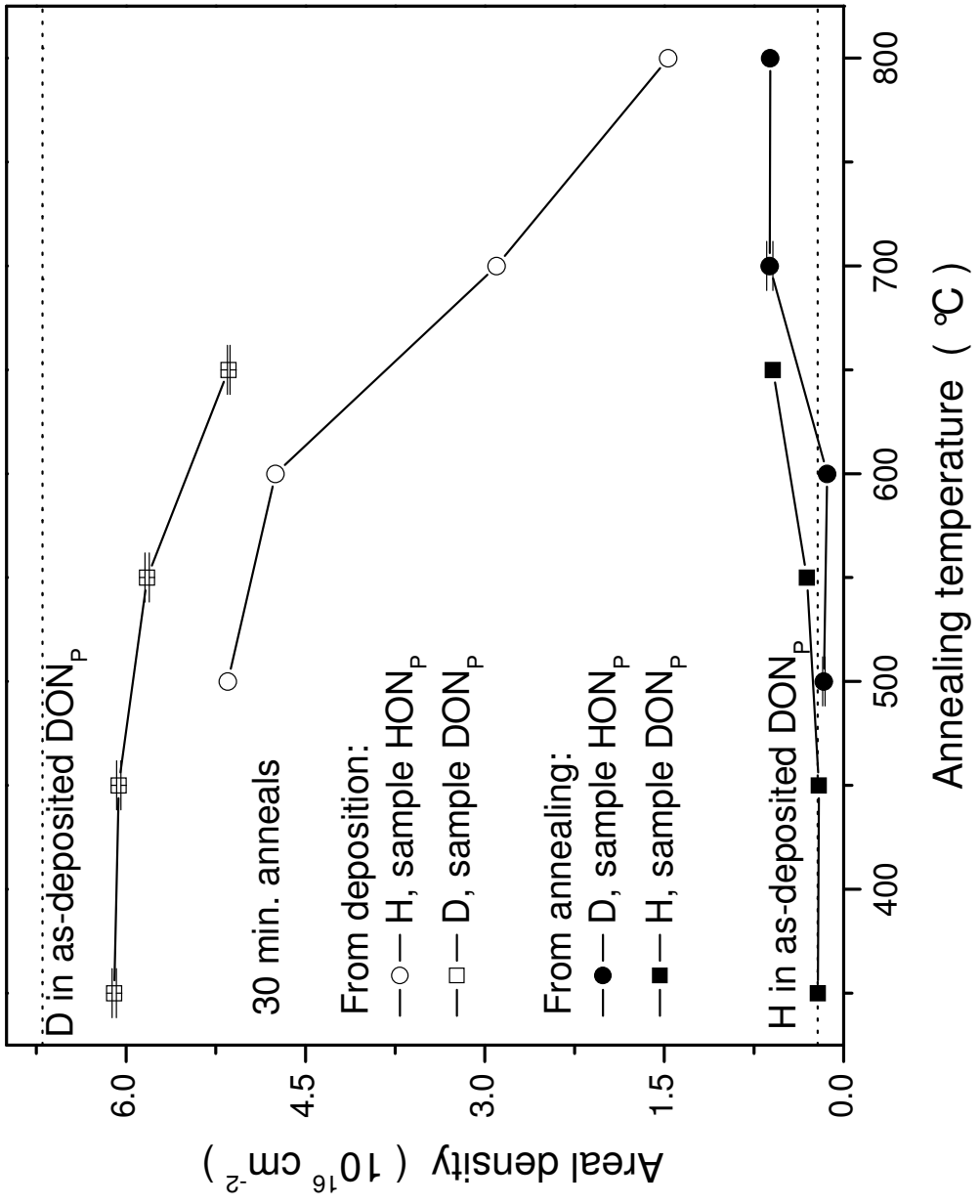
D in as-deposited DON$_P$
30 min. anneals
From deposition:
—○— H, sample HON$_P$
—□— D, sample DON$_P$
From annealing:
—●— D, sample HON$_P$
—■— H, sample DON$_P$
H in as-deposited DON$_P$
Areal density (10^{16} cm^{-2})
Annealing temperature (℃)
0.0
1.5
3.0
4.5
6.0
400
500
600
700
800

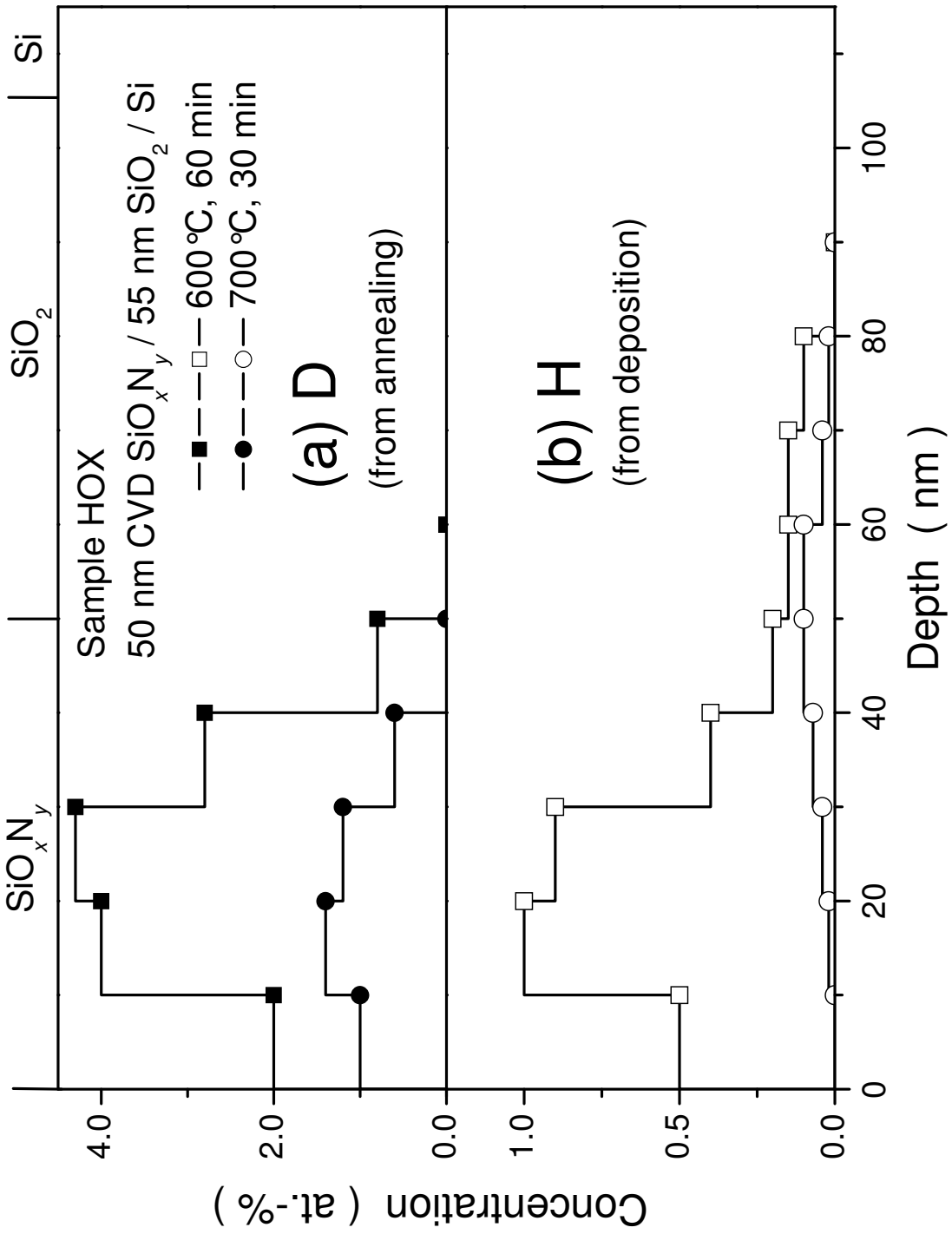
Si
SiO2
SiOxNy
Sample HOX
50 nm CVD SiOxNy / 55 nm SiO2 / Si
600 °C, 60 min
700 °C, 30 min
(a) D
(from annealing)
(b) H
(from deposition)
Concentration (at.-%)
Depth (nm)
4.0
2.0
0.0
1.0
0.5
0.0
0
20
40
60
80
100

Krug et. al., Fig. 10

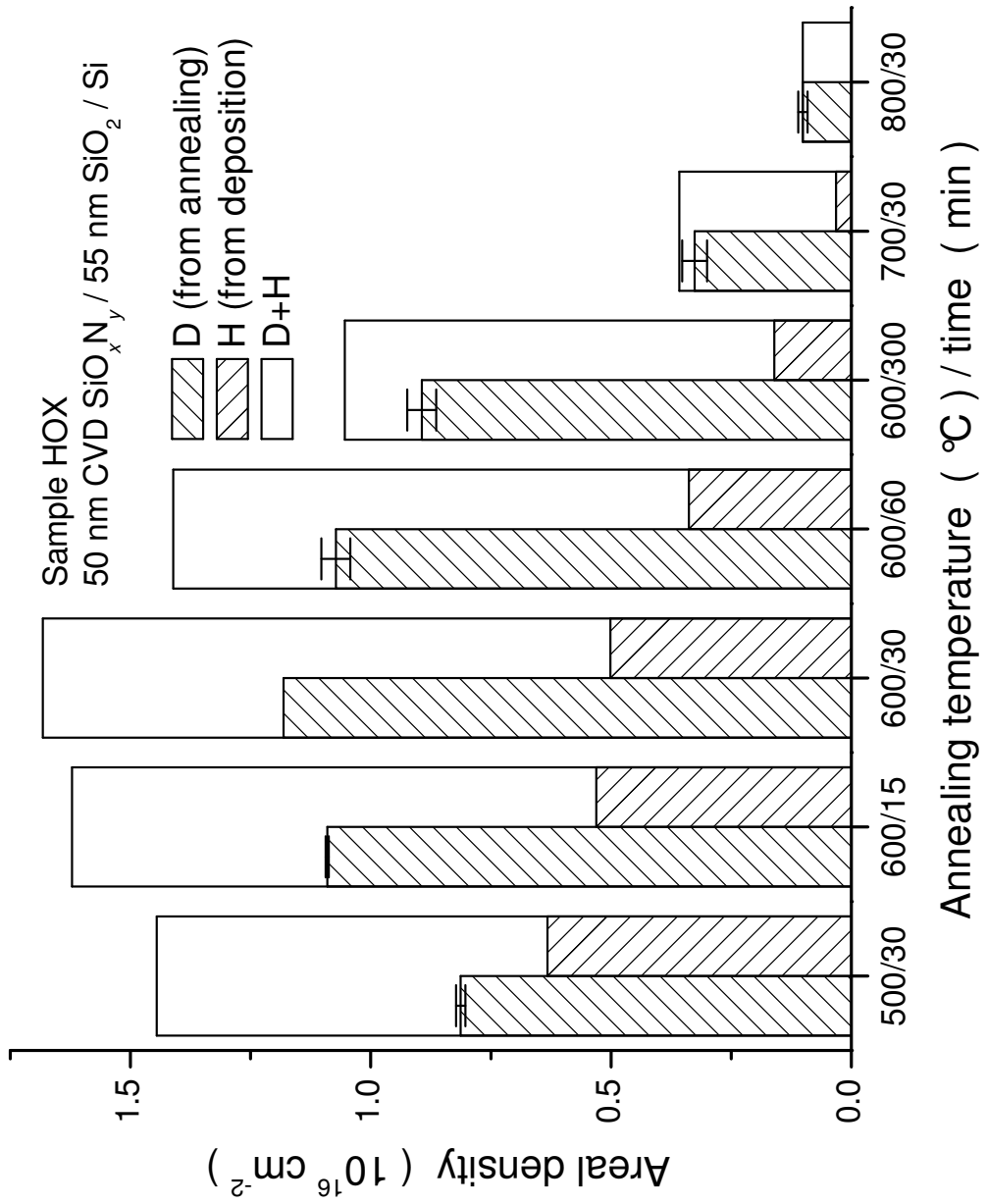

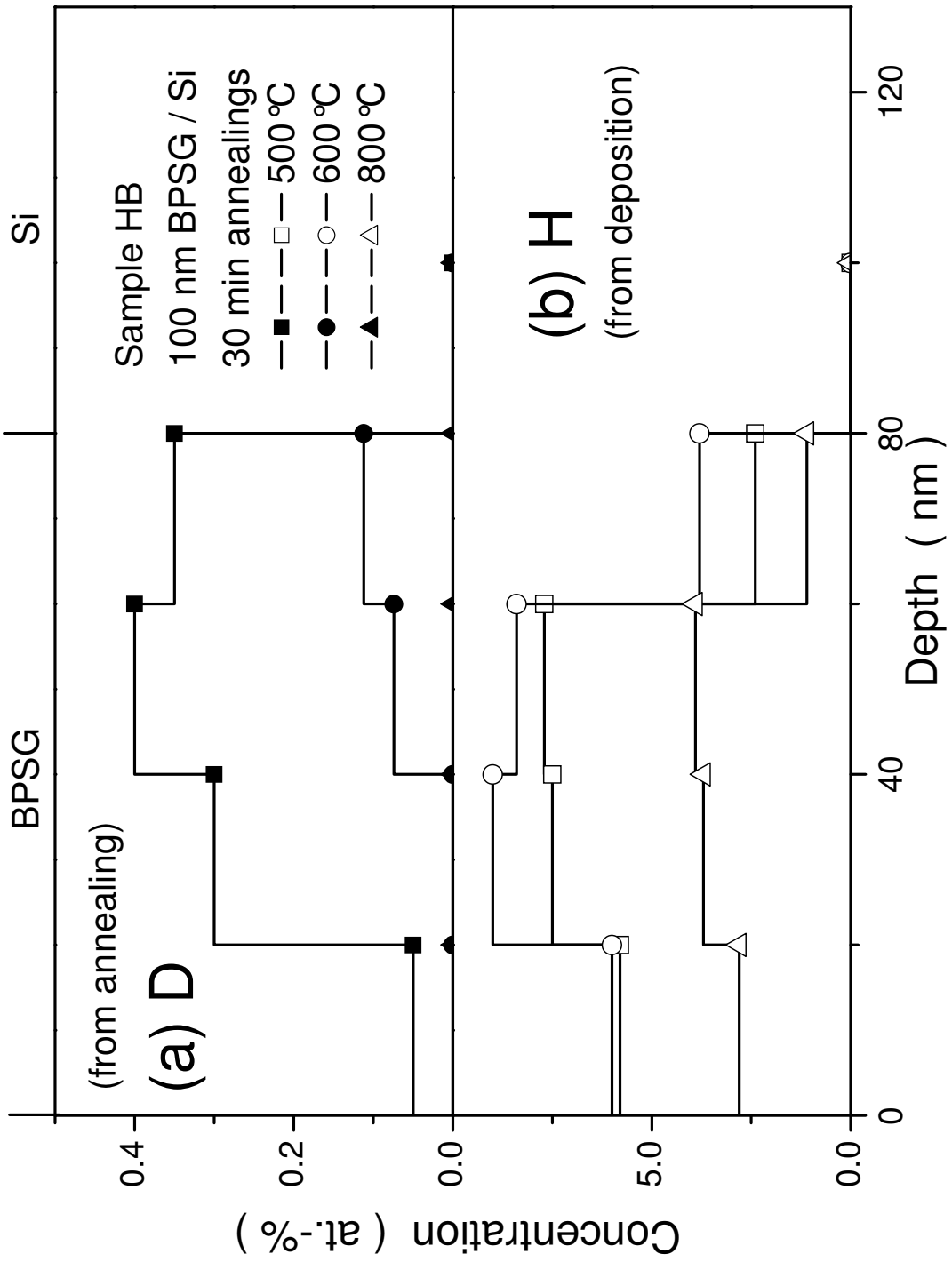
BPSG
Si
(from annealing)
(a) D
Sample HB
100 nm BPSG / Si
30 min annealings
500 °C
600 °C
800 °C
(b) H
(from deposition)
Concentration (at.-%)
Depth (nm)
0.4
0.2
0.0
5.0
0.0
0
40
80
120

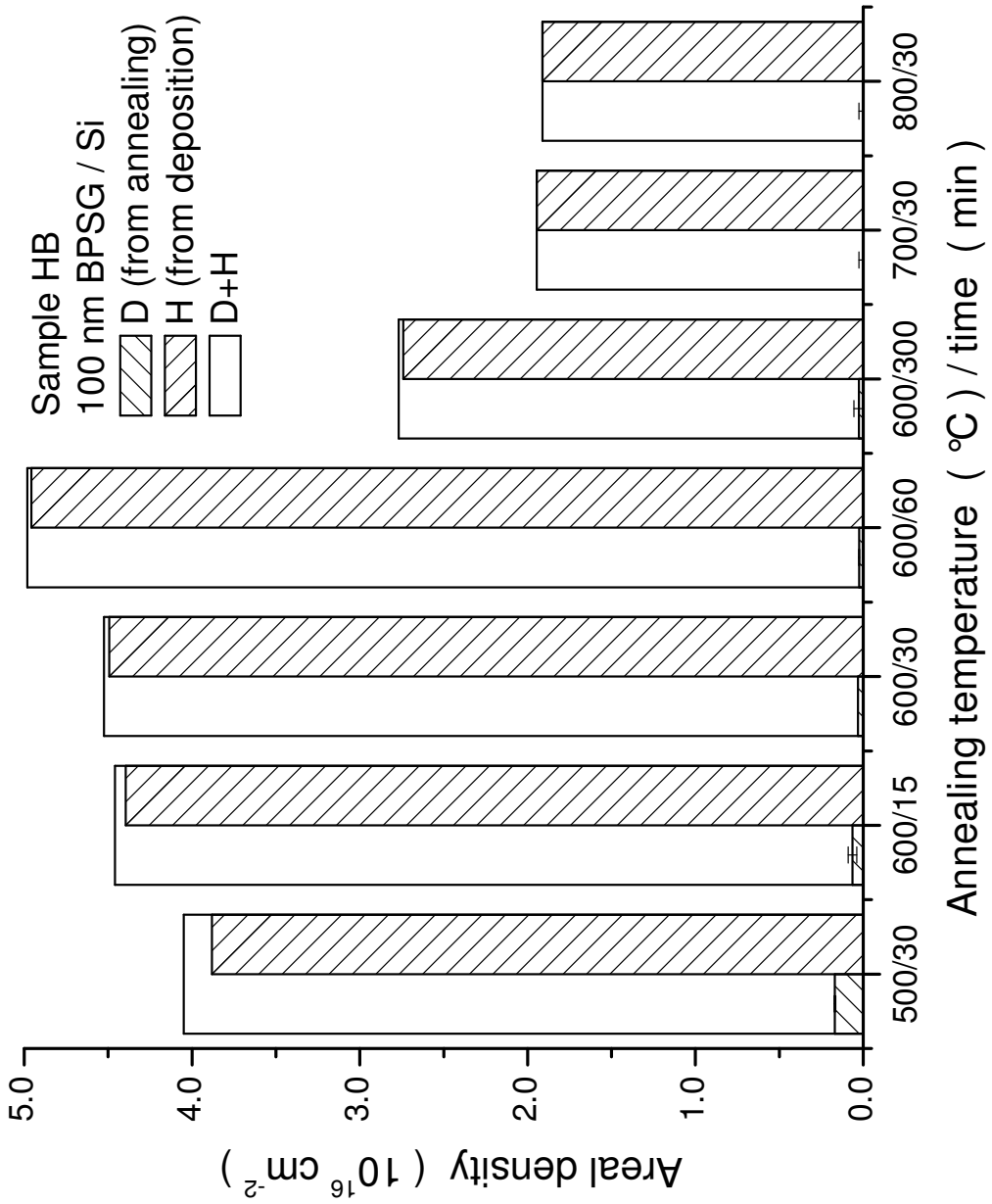
Sample HB
100 nm BPSG / Si
D (from annealing)
H (from deposition)
D+H
Areal density (10^{16} cm^{-2})
0.0
1.0
2.0
3.0
4.0
5.0
500/30
600/15
600/30
600/60
600/300
700/30
800/30
Annealing temperature (°C) / time (min)

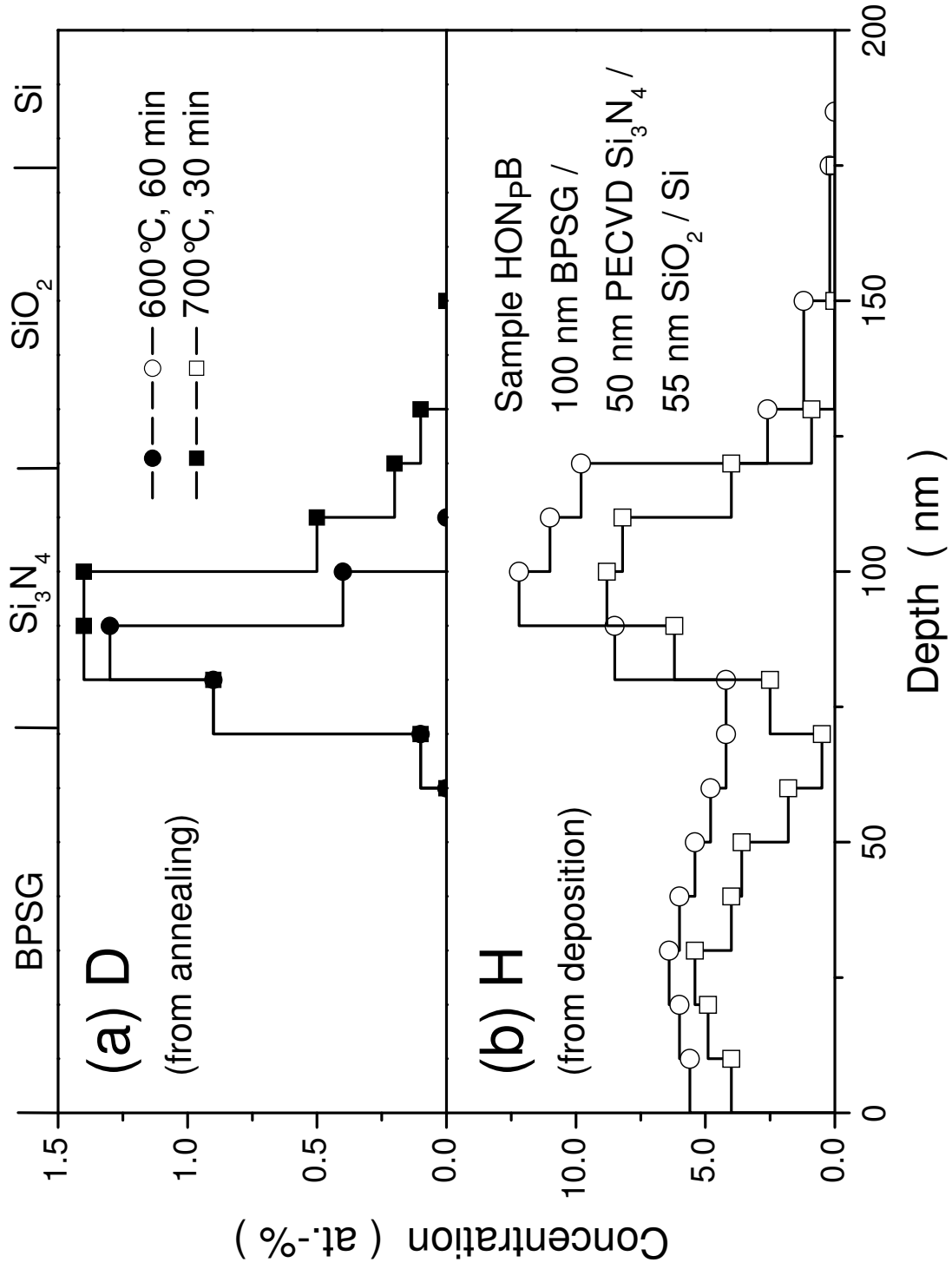
BPSG
Si3N4
SiO2
Si
(a) D
(from annealing)
600 °C, 60 min
700 °C, 30 min
(b) H
(from deposition)
Sample HONPB
100 nm BPSG /
50 nm PECVD Si3N4 /
55 nm SiO2 / Si
Concentration (at.-%)
Depth (nm)
1.5
1.0
0.5
0.0
10.0
5.0
0.0
0
50
100
150
200

Krug et. al., Fig. 14